Solar Energy Advances 2 (2022) 100016

Contents lists available at ScienceDirect

Solar Energy Advances

journal homepage: www.elsevier.com/locate/seja

On the effect of dynamic albedo on performance modelling of offshore floating photovoltaic systems

Sara Golroodbari*, Wilfried van Sark[1]

Copernicus Institute, Utrecht University, Princetonlaan 8a, 3584 CB Utrecht Utrecht, the Netherlands

ARTICLE INFO

Keywords:
Floating PV
Albedo
PV performance

ABSTRACT

In this paper, the effect of dynamic albedo on modelling energy generation of a floating offshore photovoltaic system is quantified, for a system assumed to be installed at the North Sea. The dynamic albedo is modeled as a function of solar irradiation, wind speed and solar zenith angle at an hourly time resolution. The energy output of a floating offshore PV system is compared considering two scenarios (i) implementing constant albedo and (ii) implementing a modeled dynamically varying albedo. The quantified results show that the system performance in case of a varying albedo is larger by about 1.03% compared to using a constant albedo.

1. Introduction

Solar rays pass through the atmosphere and clouds before arriving at a surface on Earth. In addition, the environment surrounding such a surface affects the radiation on that surface. To determine the irradiance that is impinging on a photovoltaic (PV) solar panel, both direct and indirect radiation must be taken into account, with direct being radiation that passes in a straight line from the sun through the atmosphere to the panel and diffuse radiation that has been scattered by atmosphere and clouds. Figure 1 illustrates the various components of solar irradiance, including reflection from objects in the environment of the panel. In this paper we focus on reflection from ocean surface water in offshore floating systems [17].

The classical approach to the modeling of reflected irradiance (R_ϕ) assumes that reflected rays are diffuse and coefficients of reflection of the direct and diffuse rays are identical [7,11]. Therefore, R_ϕ is calculated using Eq. (1):

$$R_\phi = \alpha_s \times G_h \times R_h \tag{1}$$

where α_s is the surface albedo (with subscript s denoting surface reflection, to distinguish from absorption) and $R_h = 0.5(1 - \cos\beta)$ is the transposition factor for ground reflection, with β the panel tilt angle [11]. In [2,15] seasonal and spatial albedo variation on the energy output of solar farms implementing bifacial panels has been studied. Regarding their models it is concluded that seasonal albedo variation does not lead to significant fluctuation in the energy output and a calculation based on time averaged albedo estimates the correct result accurately. In [22] authors showed that floating PV system implementing bifacial panels performs 13% higher compared to a similar system implementing monofacial panels.

In this research we aim to quantify the variation of the value of α_s for the ocean surface, considering the effect of wind and also waves for offshore floating PV systems, which provides more accurate modeling of energy yield of floating offshore PV systems [7].

Albedo is defined as a non-dimensional, unitless quantity that indicates how well a surface reflects solar energy. In the oceans, the fraction of solar radiation penetrating the subsurface is controlled by the ocean surface albedo (OSA, or α_{OSA}) [19]. Despite its importance, OSA is a parameter that receives insufficient attention from both an observational and modeling point of view and in most studies, it is assumed to be a constant ($\alpha_{OSA} \simeq 0.06$) for the open ocean surface [16]. It is also reported that the solar zenith angle (SZA) is the most prominent driving parameter for OSA, for instance in [10] several parameterisations are compared. These result in

$$\alpha_{OSA}(\zeta) = \frac{c_1}{c_2 \mu_\zeta^{c_3} + c_4} \tag{2}$$

where ζ is solar zenith angle, $\mu_\zeta = \cos(\zeta)$, and c_1, c_2, c_3, and c_4 are constants. For example, Taylor et al. [20] suggest $c_1 = 0.037$, $c_2 = 1.1$, $c_3 = 1.4$, and $c_4 = 0.15$. Consequently for this model, OSA varies between 0.0296 and 0.247 for SZA between 0 and 90 degrees. However, it should be noted that there are other parameters on which the OSA depends such as wavelength of ocean surface roughness, and atmospheric and oceanic properties [12,19].

Albedo commonly refers to the “whiteness” of a surface, with 0 meaning black and 1 meaning white. Following [19], ocean surface

* Corresponding author.
E-mail addresses: s.z.mirbagherigolroodbari@uu.nl (S. Golroodbari), W.G.J.H.M.vanSark@uu.nl (W. van Sark).
[1] ISES member.

https://doi.org/10.1016/j.seja.2022.100016
Received 21 February 2022; Received in revised form 3 June 2022; Accepted 3 June 2022
Available online xxx

Nomenclature

Symbol	Definition
α_s	Surface albedo
ζ	Solar zenith angle
ϕ	$\{\beta, \gamma\}$
v	Wind speed
$n(\lambda)$	Refractive index of seawater
σ	Sea surface roughness
DIR	Direct component
f_{WC}	Fraction of whitecaps
f_{DIR}	Direct fractions in GTI
β	Panel tilt angle
ξ	Incident angle
γ	Azimuth angle
λ	Wavelength
r_F	Fresnel reflectance
R	Reflected component
DIF	Diffuse component
$\alpha_W(\lambda)$	Absorption coefficient of clear water
f_{DIF}	Diffuse fractions in GTI

albedo α_{OSA} can be defined as shown in Eq. (3) [3,4,12].

$$\alpha_{OSA} = Fr_{DIR} \times \alpha_{O,DIR} + Fr_{DIF} \times \alpha_{O,DIF} \tag{3}$$

where $Fr_i, \alpha_{O,i}\ i \in \{DIR, DIF\}$ refer to the fraction of incident radiation and surface albedo, respectively, for direct and diffuse irradiation components. This fraction is computed in [3] by considering the relation between $\alpha_{O,DIR}$ and $\alpha_{O,DIF}$ as shown in Eq. (4).

$$\alpha_{O_{DIR}} = \alpha_{O_{DIF}} \times \frac{1+d}{1+2d\mu_\zeta} \tag{4}$$

where d is a parameter which is adjusted to obtain the observed surface albedo for a certain solar zenith angle. Referring to [3] the value for d varies depending on the type of surfaces, for instance for arable land, grassland and desert it is estimated to be 0.4, and for other surfaces it can be estimated to be 0.1. Therefor, considering the effect of zenith angle in Eq. (4) for the system assumed on the North Sea we can modify Eq. (4) to $\alpha_{O_{DIR}} \approx (\alpha_{O_{DIF}} \pm 0.1 \times \alpha_{O_{DIF}})$. Hence, as the variation on the total albedo in this study is negligible we assumed the direct-to-diffuse fraction of downwelling radiation to equal one, and separate the ocean surface albedo into equal direct ($\alpha_{O,DIR}$) and diffuse ($\alpha_{O,DIF}$) contributions. Moreover, reflectively of the ocean surface is not only depending on the intrinsic spectral reflectively on the surface of the water, but also depends on the fraction of direct to diffuse irradiance from the atmosphere. This study includes also a second effect: given the wind speed, surface roughness and zenith angle, $\alpha_{O,DIR}$ and $\alpha_{O,DIF}$ can be calculated explicitly, which will be explained in the following sections. A mathematical model developed by Cox and Munk [5] is implemented in this research which estimates a function to parameterise the mean contribution of multiple reflective facets at the ocean surface. This polynomial function is given in Section 2.3.

In this paper we will study the effect of wind speed on surface ocean albedo. Gordon and Jacobs [8] separate the effect of wind speed in two different and opposite effects: (i) the albedo of the surface decreases only slightly with increasing wind speed while this leads to increased roughness, (ii) further increasing the wind speed over the ocean, however, results in another process which increases the surface albedo: the formation of white caps. The effect of wind is not a simple linear effect. Therefore, we need to study in more detail how the variation in the wind speed could change the surface ocean albedo and how this affects energy yield estimations for offshore PV, as is described earlier [7].

In the rest of paper, first we will discuss the mathematical model for quantifying the surface ocean albedo value in Section 2. In Section 3 we will compare the results from this model for the estimation of PV energy yield in comparison to the use of a constant albedo value. Finally, we will wrap up the paper with a conclusion in Section 4.

2. Methodology

The global irradiation on a tilted surface (GTI) determines the power generated by a PV panel. It is calculated using Eq. (5) [7]:

$$GTI = DIR_{\phi,\zeta} + DIF_{\phi,\zeta} + R_{\phi,\zeta} \tag{5}$$

where DIR_ϕ, DIF_ϕ and $R_{\phi,\zeta}$ are direct, diffuse, and reflective irradiance components, respectively, and $\phi = \{\beta, \gamma\}$ where β is surface tilt angle and γ is azimuth angle, and ζ is solar zenith angle.

As mentioned in the introduction the classical approach to model $R_{\phi,\zeta}$ assumes that reflected radiation is isotropic and coefficients of reflection of the direct and diffuse rays are identical [9]; therefore, $R_{\phi,\zeta}$ is calculated using Eq. (1). However, such a surface is called Lambertian and there exists no surface with this characteristics. All surfaces have internal elements with sizes comparable to the wavelengths of incident sunlight scattering light and contribute to the light reflected by the surface. In the oceans, minuscule variations in density, air bubbles, particles of sand and dust, organic compounds, and microscopic organisms all give rise to scattered light [4].

Albedo $\alpha \in [0, 1]$ is a non-dimensional, unitless quantity that indicates how well a surface reflects solar irradiance. It is reported that albedo for an open ocean α_{OSA} depends on a number of parameters,

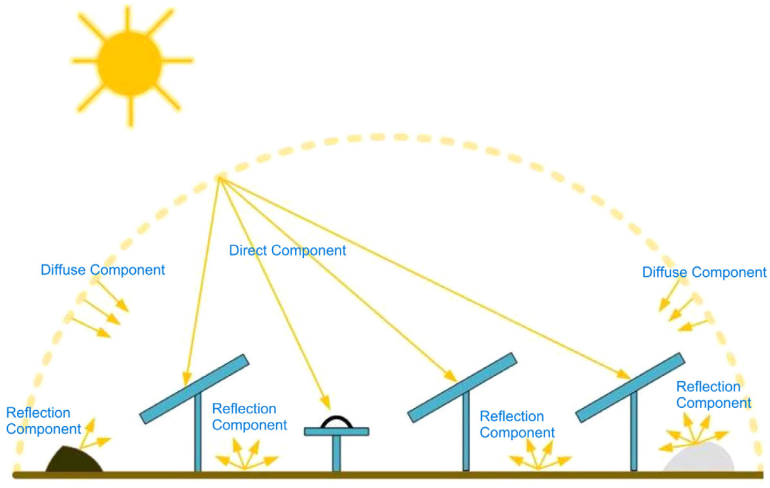

Fig. 1. Solar irradiance components, direct, diffuse and reflection.

which include several atmospheric and oceanic properties, solar zenith angle (ζ), ocean surface roughness, which itself is a function of wind speed, and optical wavelength [12]. The incident solar radiation namely direct and diffuse, is first influenced by the presence of whitecaps, which exhibits different reflective properties from seawater. Then, the reflective properties of the uncapped fraction of the sea surface are determined separately for direct and diffuse incident radiation [19]. In this research for simplicity we neglect the effect of the subsurface or the ocean interior.

2.1. Whitecaps

The fraction of whitecaps (f_{WC}) can be generated from the disturbance coming from the breaking of waves due to the wind. This turbulence generates the foam at the sea surface which can change the albedo considerably [6,19]. In this work, we use Eq. (6) to formulate the f_{WC} as a function of wind speed (v [m/s]) at height of 10 m above the sea surface [18].

$$f_{WC}(v) = 3.97 \times 10^{-2} \times v^{1.59} \quad | \quad v \in [2 \quad 20] m/s \tag{6}$$

Equation (7) is proposed in [23] as a polynomial relationship for solar spectral dependence of $\alpha_{s,f_{WC}}$.

$$\alpha_{s,f_{WC}}(\lambda) = \frac{0.5}{100}\Big[60.063 - 5.127 \ln \alpha_W(\lambda) + 2.799\big(\ln \alpha_W(\lambda)\big)^2 - 0.713\big(\ln \alpha_W(\lambda)\big)^3 + 0.044\big(\ln \alpha_W(\lambda)\big)^4\Big] \tag{7}$$

where $\alpha_W(\lambda)$ is the absorption coefficient of clear water in m^{-1}. In this research the $\alpha_W(\lambda)$ values which are published in both [19,23] are used for $\lambda \in [400 \quad 2400]$ nm. As discussed in [13,19] the fraction of whitecaps' albedo $\alpha_{s,f_{WC}}(\lambda)$, tends to be twice as small as that of fresh and dense foam; therefore, the coefficient of 0.5 is added to the formulation proposed by Whitlock et al. [23].

2.2. The roughness of the sea surface

An absolutely calm sea surface reflects the sun like a mirror at the horizontal specular point. However, usually there are thousands of "dancing" highlights. At each highlight there is a water facet, possibly quite small, which is so inclined as to reflect an incoming ray from the sun towards the observer [5]. Regarding this fact the roughness of the sea surface, so called σ, is estimated in Eq. (8) [5]. showing the dependence on wind speed.

$$\sigma^2 = 0.003 + 0.00512v \tag{8}$$

2.3. Fresnel surface albedo for direct and diffuse components

The major components of α_{OSA} are described by Eqs. (9) and (11) which are the contribution of Fresnel reflection at the ocean surface.

$$\alpha_{O,DIR}(\lambda, \xi, \omega) = r_F(n(\lambda), \mu) - \frac{r_F(n(\lambda), \mu)}{r_F(n_0, \mu)} \times f(\mu, \sigma) \tag{9}$$

where $\mu = \cos(\xi)$, with ξ the incident angle, $n(\lambda)$ is the wavelength dependent refractive index of seawater, r_F is the Fresnel reflectance for a flat surface and $f(\mu, \sigma)$ is a function that accounts for the distribution of multiple reflective facets at the ocean surface estimated in the visible spectrum (VIS). Values for variable $n(\lambda)$ are extracted from [12,19]. Also, it is assumed that $n_0 = 1.34$ calculated from the refractive index of seawater averaged in the VIS. Function $f(\mu, \sigma)$ is found from multiple regression in [12] as follows:

$$f(\mu, \sigma) = \big(0.0152 - 1.7873\mu + 6.8972\mu^2 - 8.5778\mu^3 + 4.071\sigma - 7.644\mu\sigma\big) \times \exp(0.1643 - 7.8409\mu - 3.5639\mu^2 - 2.3588\sigma + 10.0538\mu\sigma) \tag{10}$$

A simple expression for the calculation of α_{DIF} is implemented in this research using only surface roughness and refractive index as variables [12]:

$$\alpha_{O,DIF}(\lambda, \sigma) = -0.1479 + 0.1502n(\lambda) - 0.0176n(\lambda)\sigma \tag{11}$$

Considering the components of total OSA, i.e. $\alpha_{O,DIR}$ and $\alpha_{O,DIF}$, we calculate the total OSA using the ratio of direct and diffuse irradiation, considering the assumption in Eq. (3):

$$\alpha_{OSA} = f_{DIR}\alpha_{O,DIR} + f_{DIF}\alpha_{O,DIF} \tag{12}$$

with f_{DIR} and f_{DIF} the direct and diffuse fractions in GTI, respectively. Like $\alpha_{O,DIR}$ and $\alpha_{O,DIF}$ these are wavelength dependent and are shown in Eq. (13). For simplicity in this research the contribution of the ocean interior reflectance to the ocean surface albedo is neglected [19].

$$\begin{aligned} \alpha_{O,DIR}(\lambda, \zeta, v) &= \alpha_{O,DIR} \times (1 - f_{WC}(v)) + f_{WC}(v)\alpha_{R f_{WC}}(\lambda) \\ \alpha_{O,DIF}(\lambda, \zeta, v) &= \alpha_{O,DIF} \times (1 - f_{WC}(v)) + f_{WC}(v)\alpha_{R f_{WC}}(\lambda) \end{aligned} \tag{13}$$

Regarding Eq. (13) the effect of whitecaps on the direct and diffuse albedo is formulated with $(1 - f_{WC})$ as coefficient which means that when f_{WC} is increasing the effect of whitecaps on albedo is becoming dominant. Finally, the sea surface albedo α_{OSA} is calculated using Eq. (3).

2.4. PV system

We develop a model of a small FPV system consisting of 12 identical silicon panels, having a total system capacity of 3.72 kWp. The panels are assumed to be placed on a steel pontoon that is fixed with four wire ropes to four buoys in its surroundings. The wire ropes limit the degree of freedom for the pontoon, in this way dealing with impact from sea waves. Hence, tilt angles are restricted to 20 degrees at maximum.

3. Results and discussions

In this section we will present and review the results in detail. The results which will be discussed hereafter are extracted from implementing the albedo model discussed in this paper in the mathematical model developed in [7]. The mathematical model for the offshore floating PV system considers the following variables: (i) irradiation, (ii) wind speed, and (iii) relative humidity. For this model we considered variable tilt angles implementing Joint North Sea Wave Project (JONSWAP) spectra, as detailed in [7]. Data at hourly time resolution in this paper is from the Royal Netherlands Meteorological Institute (Koninklijk Nederlands Meteorologisch Instituut) website [21].

Output energy for the same system is compared in two scenarios as follows: (i) with constant $\alpha_{OSA} = 0.06$ as is calculated as the albedo for the open ocean surface reported by the American National Snow and Ice Data [1], and (ii) according to the more precise method as discussed in the methodology section to calculate albedo dynamically using wind speed and ζ. At first, we will discuss the relation between wind speed and albedo and after that we will review the difference between energy yield for the year 2016 considering constant and modeled albedo.

Figure 2 (a,b) shows box plots of the daily variation of albedo and the wind speed during January and August 2016, respectively. These two months are chosen as examples to depict the time trend of both wind speed and albedo during one month with much higher solar zenith angle values in August compared to January. The average value for albedo in January is $\overline{\alpha}_{OSA,Jan} = 0.25$ which is 0.044 higher than the value in August $\overline{\alpha}_{OSA,Aug} = 0.206$. Note, these are considerably larger compared to the constant albedo of 0.06. Two main results may be concluded regarding this figure, (i) when the solar zenith angle is higher the average value for albedo is also higher, (ii) the trend of the wind speed is not completely followed by the albedo value trend in these two months.

For a deeper view let us discuss the whole year. Figure 3 shows the scatter plots for daily averages of albedo and wind speed for all 12

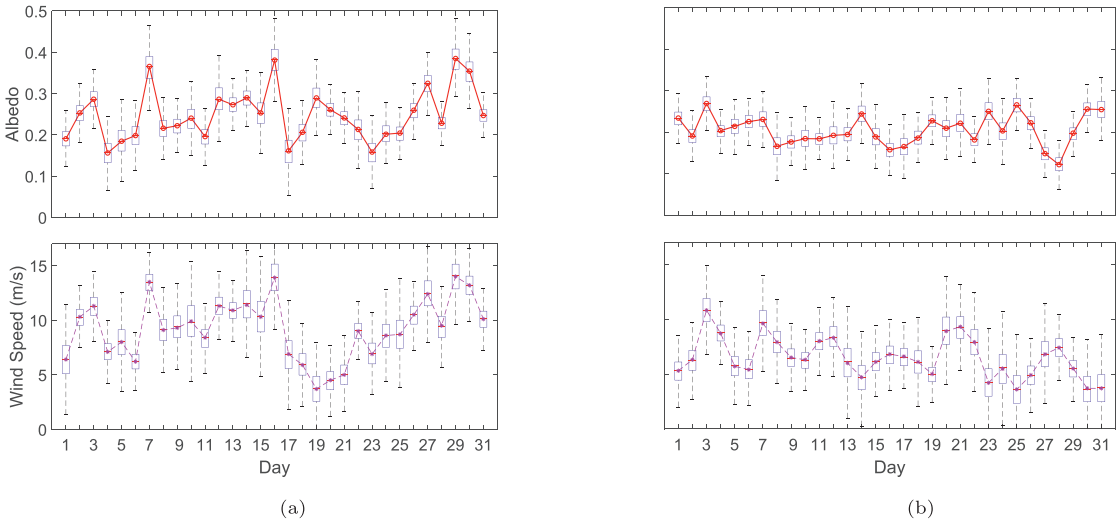

Fig. 2. Daily averaged albedo and wind speed (m/s) implementing time resolution data for 2016, (a) January (b) August.

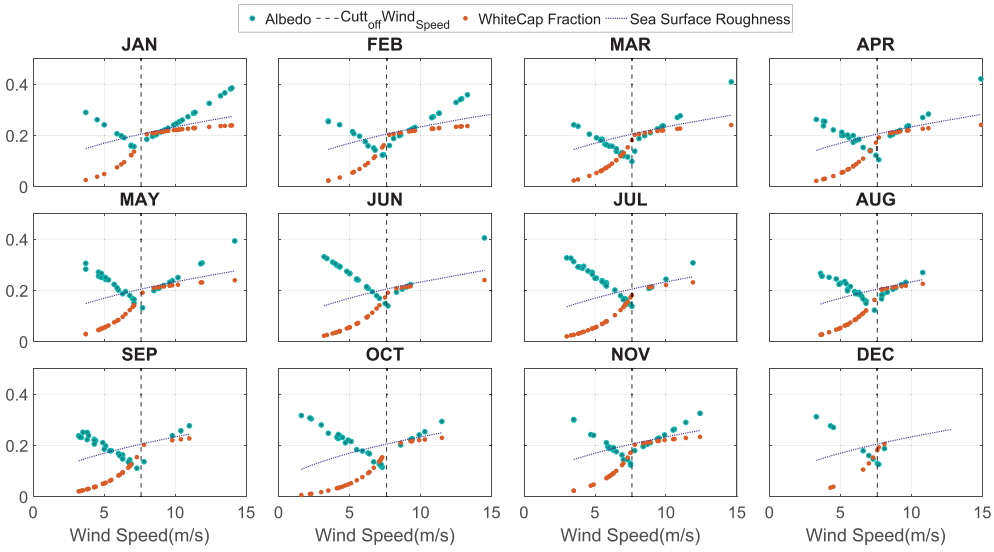

Fig. 3. Scatter plots of albedo and whitecap fraction as a function of wind speed for the year 2016. For the threshold wind speed value (dashed line), see text.

months of the year 2016, and also the behaviour of sea surface roughness. This figure shows that albedo is larger in winter months compared to summer months and also the wind speed does not necessarily only increase the albedo value. Increasing the wind speed leads to larger sea surface roughness and decreasing albedo, however, by exceeding a certain threshold value for the wind speed the albedo starts increasing again. This is due to the formation of white caps on the sea surface which are more clearly visible during months with larger solar zenith angle. As shown in Fig. 3 there is a threshold point from which the effect of whitecaps starts dominating the sea surface roughness. This threshold value which shows the change in behaviour due to wind speed, can be easily found by considering the followings:

$$1 - f_{WC} = 1 - (3.97 \times 10^{-2} \times v^{1.59}) = 0 \tag{14}$$

Equation (14) gives $v = 7.61$ m/s, which is shown in Fig. 3 using a dashed dotted line.

Using the albedo data presented here in the performance model simulation [7], we arrive at the results shown in Fig. 4. Figure 4 shows the output difference in % for the energy yield of a floating PV system for the two different albedo scenarios for data of the year 2016 at Hoek van Holland (southwest of the Netherlands). It can be concluded that taking into account a varying albedo, the calculated PV system performance is larger in all months throughout the year, with an annual average of about 1.03%, without a clear seasonal effect, compared to using a fixed value for α_{OSA}.

Increased performance is due to increased GTI. Figure 5 shows the ΔGTI shown in Eq. (15) comparing varying and constant albedo, calculated using Eq. (15), and 2016 KNMI data.

$$\Delta GTI = GTI_{modeled\ albedo} - GTI_{constant\ albedo} \tag{15}$$

Summing the months, annual GTI would be 14.8 kWh/m^2 higher if we consider the albedo with the studied mathematical model in this paper. This difference will lead to an increase of 13.4 kWh/kWp which is equal to 1.03% difference in performance in our modeled offshore FPV system. The annual energy yield computed by our FPV model is 1346 kWh/kWp. Considering the dynamic albedo modeling this value changed to 1359.4 kWh/kWp. The rather small increase in performance due to including dynamically varying albedo can be understood realizing that the floating PV system is mounted horizontally in the water. The panel tilt is limited to 20° and we have shown in [7] that tilt angles are rarely above 10° only in case of high wind speeds. Additional reflected irradiation on horizontally located PV panels thus is limited. It can be expected that floating PV systems that are installed having a permanent non-zero tilt, will benefit more from including dynamically

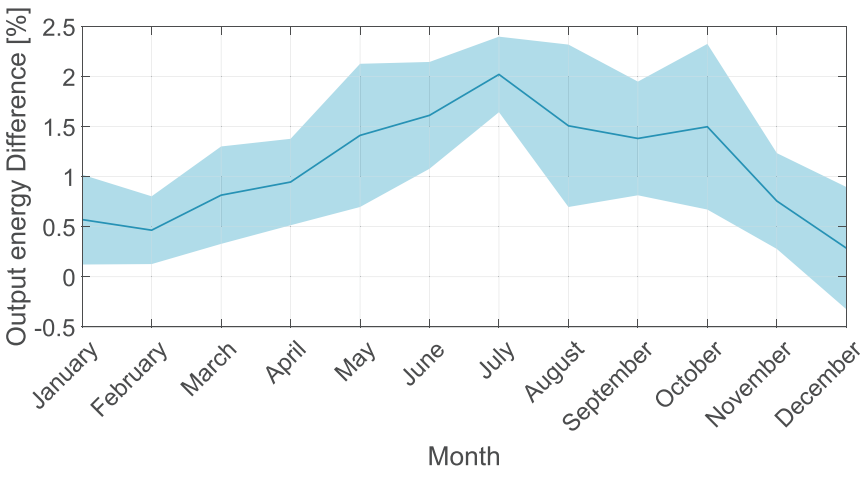

Fig. 4. The output energy relative difference in % between the system implementing a modeled albedo and a constant albedo for the location of the system. The line shows the means of the monthly datasets, while the upper and lower bounds show the standard deviations in the data.

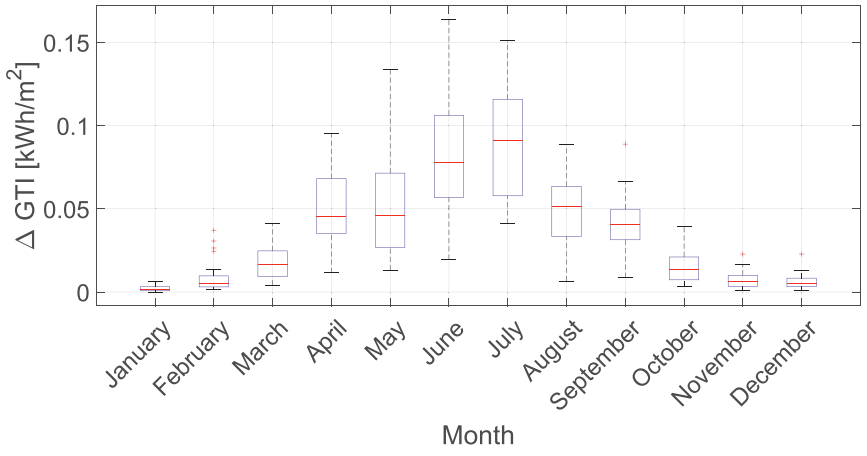

Fig. 5. The increase in surface irradiation considering modeled albedo and constant albedo.

varying albedo, while it should be noted that increased performance of bifacial floating PV systems has been reported to be limited [14].

4. Conclusion

In this paper, first a mathematical model for sea surface albedo is presented. It should be noted that the contribution of the ocean interior reflecting to surface albedo is neglected in this model. The modeled albedo is implemented in a fully mathematical performance model of an offshore floating PV system considering variable tilt due to the wave spectrum and wind speed. The results showed that albedo does not have a simple linear relation with wind speed. If the wind is strong enough to form whitecaps the albedo starts increasing and sea surface roughness is not dominant anymore. Comparing the floating PV system implementing constant and modeled albedo shows that compared to a fixed value for α_{OSA}, the PV system performance is larger by about 1.03% on average, without clear seasonal differences. Although this significant difference is coming from the behaviour of the wind in the considered data and location, this shows that dynamic albedo should be used in performance evaluations of floating PV systems. Moreover, it should be taken into consideration that the average difference may change for different years and different locations.

Declaration of Competing Interest

It is with great pleasure to submit a research paper to the esteemed journal Solar Energy Advances, entitled:

"On the Effect of Dynamic Albedo Modeling of Offshore Floating Photovoltaic Systems".

We confirm that this manuscript has not been submitted nor published elsewhere and have no conflicts of interest to declare.

We sincerely hope that the paper in its present or revised form can be accepted for publication.

Acknowledgements

This work is partly financially supported by the Netherlands Enterprise Agency (RVO) within the framework of the Dutch Topsector Energy (project Comparative assessment of PV at Sea versus PV on Land, CSEALAND).

References

[1] American national snow and ice data (NSID), http:https://nsidc.org.
[2] R. Bailey, P. Keelin, R. Perez, J. Robinson, G. Bender, J. Chard, Investigations of site-specific, long term average albedo determination for accurate bifacial system energy modeling, in: 2019 IEEE 46th Photovoltaic Specialists Conference (PVSC), IEEE, 2019, pp. 2268–2274.
[3] B.P. Briegleb, P. Minnis, V. Ramanathan, E. Harrison, Comparison of regional clear-sky albedos inferred from satellite observations and model computations, J. Appl. Meteorol. Climatol. 25 (2) (1986) 214–226. https://journals.ametsoc.org/view/journals/apme/25/2/1520-0450_1986_025_0214_corcsa_2_0_co_2.xml.
[4] J. Coakley, Reflectance and albedo, surface, Encycl. Atmos. 1 (2003) 1914–1923.
[5] C. Cox, W. Munk, Measurement of the roughness of the sea surface from photographs of the sun's glitter, J. Opt. Soc. Am. 44 (11) (1954) 838–850.
[6] R. Frouin, M. Schwindling, P.-Y. Deschamps, Spectral reflectance of sea foam in the visible and near-infrared: in situ measurements and remote sensing implications, J. Geophys. Res. 101 (C6) (1976) 14361–14371, doi:10.1029/96JC00629.
[7] S.Z. Golroodbari, W. van Sark, Simulation of performance differences between offshore and land-based photovoltaic systems, Prog. Photovoltaics Res. Appl. 28 (9) (2020) 873–886.
[8] H.R. Gordon, M.M. Jacobs, Albedo of the ocean–atmosphere system: influence of sea foam, Appl. Opt. 16 (8) (1977) 2257–2260.

[9] M. Gulin, M. Vašak, M. Baotic, Estimation of the global solar irradiance on tilted surfaces, in: 17th International conference on electrical drives and power electronics (EDPE 2013), vol. 6, 2013, pp. 347–353.
[10] C.J. Huang, F. Qiao, S. Chen, Y. Xue, J. Guo, Observation and parameterization of broadband sea surface albedo, Journal of Geophysical Research: Oceans 124 (2019) 4480–4491.
[11] P. Ineichen, A. Zelenka, O. Guisan, A. Razafindraibe, Solar radiation transposition models applied to a plane tracking the sun, Sol. Energy 41 (4) (1988) 371–377.
[12] Z. Jin, Y. Qiao, Y. Wang, Y. Fang, W. Yi, A new parameterization of spectral and broadband ocean surface albedo, Opt. Express 19 (27) (2011) 26429–26443, doi:10.1364/OE.19.026429.
[13] P. Koepke, Effective reflectance of oceanic whitecaps, Appl. Opt. 23 (11) (1984) 1816–1824.
[14] H. Liu, V. Krishna, J. Lun Leung, T. Reindl, L. Zhao, Field experience and performance analysis of floating PV technologies in the tropics, Prog. Photovoltaics Res. Appl. 26 (12) (2018) 957–967, doi:10.1002/pip.3039.
[15] M.T. Patel, M.R. Khan, A. Alnuaimi, O. Albadwawwi, J.J. John, M.A. Alam, Implications of seasonal and spatial albedo variation on the energy output of bifacial solar farms: a global perspective, in: 2019 IEEE 46th Photovoltaic Specialists Conference (PVSC), IEEE, 2019, pp. 2264–2267.
[16] R.E. Payne, Albedo of the sea surface, J. Atmos. Sci. 29 (5) (1972) 959–970, doi:10.1175/1520-0469(1972)029<0959:AOTSS>2.0.CO;2.
[17] M. Rosa-Clot, G.M. Tina, Submerged and Floating Photovoltaic Systems: Modelling, Design and Case Studies, Academic Press, 2017.
[18] D.J. Salisbury, M.D. Anguelova, I.M. Brooks, Global distribution and seasonal dependence of satellite-based whitecap fraction, Geophys. Res. Lett. 41 (5) (2014) 1616–1623, doi:10.1002/2014GL059246.
[19] R. Séférian, S. Baek, O. Boucher, J.-L. Dufresne, B. Decharme, D. Saint-Martin, R. Roehrig, An interactive ocean surface albedo scheme (OSAv1. 0): formulation and evaluation in ARPEGE-Climat (V6. 1) and LMDZ (V5A), Geosci. Model Dev. 11 (2018) 321–338.
[20] J.P. Taylor, J.M. Edwards, M.D. Glew, P. Hignett, A. Slingo, Studies with a flexible new radiation code. II: comparisons with aircraft short-wave observations, Q. J. R. Meteorol.Soc. 122 (1996) 839–861.
[21] The Royal Netherlands Meteorological Institute, Dutch National Weather Service, 2022, https://www.knmi.nl.
[22] G.M. Tina, F.B. Scavo, L. Merlo, F. Bizzarri, Comparative analysis of monofacial and bifacial photovoltaic modules for floating power plants, Appl. Energy 281 (2021) 116084.
[23] C.H. Whitlock, D.S. Bartlett, E.A. Gurganus, Sea foam reflectance and influence on optimum wavelength for remote sensing of ocean aerosols, Geophys. Res. Lett. 9 (6) (1982) 719–722, doi:10.1029/GL009i006p00719. (1082)